IEEE Photonics Journal
An IEEE Photonics Society Publication

Open Access

A Compact and Temperature-Sensitive Directional Coupler Based on Photonic Crystal Fiber Filled With Liquid Crystal 6CHBT

Volume 4, Number 5, October 2012

Dora Juan Juan Hu
Perry Ping Shum
Jun Long Lim
Ying Cui
Karolina Milenko
Yixin Wang
Tomasz Wolinski

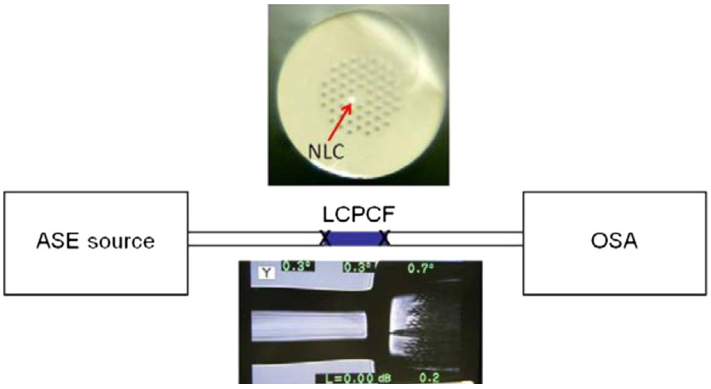

DOI: 10.1109/JPHOT.2012.2223662
1943-0655/$31.00 ©2012 IEEE

IEEE photonics SOCIETY

IEEE

A Compact and Temperature-Sensitive Directional Coupler Based on Photonic Crystal Fiber Filled With Liquid Crystal 6CHBT

Dora Juan Juan Hu,[1,2] Perry Ping Shum,[3,4] Jun Long Lim,[1,3] Ying Cui,[3,4] Karolina Milenko,[1,3,5] Yixin Wang,[1] and Tomasz Wolinski[5]

[1]RF&Optical Department, Institute for Infocomm Research, Singapore 138632
[2]Wellman Center for Photomedicine, Massachusetts General Hospital, Boston, MA 02114 USA
[3]School of Electrical and Electronics Engineering, Nanyang Technological University, Singapore 639798
[4]CINTRA CNRS/NTU/THALES, Singapore 639798
[5]Faculty of Physics, Warsaw University of Technology, 00-661 Warsaw, Poland

DOI: 10.1109/JPHOT.2012.2223662

Manuscript received September 15, 2012; revised October 5, 2012; accepted October 5, 2012. Date of publication October 9, 2012; date of current version October 16, 2012. This work was supported in part by the A*STAR, Singapore, through the SERC Thematic Strategic Research Program (TSRP) under Grant 102-152-0012. Corresponding author: P. P. Shum (e-mail: shum@ieee.org).

Abstract: A directional coupler structure formed by a nematic liquid crystal (NLC)-filled photonic crystal fiber (PCF) represents a promising configuration in sensing applications. Because of large refractive index difference between the NLC and silica material, the mode coupling between the NLC waveguide and the silica core is more complicated than the situation of coupling between two fundamental modes of the waveguides. Therefore, it is necessary to perform a theoretical investigation of the mode properties associated with the experimental studies of the coupling characteristics. In this paper, we present a thorough analysis, both theoretically and experimentally, of the directional coupler structure, including the mode properties, coupling characteristics, and thermal sensing properties. The temperature response of the device is experimentally measured, showing a polynomial curve in nematic phase and a linear curve in isotropic phase. The nonlinearity of the temperature response of the device in nematic phase and the linearity in isotropic phase are attributed to the temperature dependence of the refractive index of the NLC. Specifically, the sensitivity is -3.86 nm/°C in isotropic phase of the 6CHBT with good linearity and shows good agreement with simulation results.

Index Terms: Nematic liquid crystal (NLC), photonic crystal fiber (PCF), temperature sensor, selective infiltration.

1. Introduction

The growing interest and effort in research and development of photonic crystal fibers (PCFs) and PCF-based devices and applications are primarily due to the great flexibility in controlling and manipulating the electromagnetic radiation in the tailored microstructure. In addition, the continuing improvement in PCF fabrication technology plays an important role in enabling the realization of many unique and practical PCF applications, such as supercontinuum generation source [1], high power delivery [2], medical imaging [3], optical communication components [4]–[6], optical sensing [7]–[10], etc. Furthermore, the optical properties of the PCFs can be effectively modified, and therefore, acquiring additional functionalities by filling the air holes with polymer [11], gas [12], liquid [13],

metal [14], and semiconductor [15]. In this regard, PCFs act as light conduits and promising platforms to integrate thermooptic, optofluidic, and optoelectronic technologies for developing multi-functional devices. The pioneering work of liquid-filled PCF has demonstrated versatility in sensing applications and optical properties engineering such as birefringence and nonlinearity [16]–[19]. By selectively filling liquid to a single void in the cladding, a PCF directional coupler structure can be formed [20], [21]. The liquid crystal (LC)-filled PCF (LCPCF) has demonstrated useful tunable properties for various applications such as switching [22], attenuator [23], and sensing [24] *via* electric, optical, or thermal control. The reported LCPCF structures predominately fill LC materials in all air holes of the fiber and, hence, change the guiding mechanism of PCF from modified total internal reflection to photonic bandgap guidance due to higher refractive indices of the LC material. As a result, the bandgap properties can be controlled and utilized for sensing purposes [25], [26]. However, through our experimental studies, we have found that infiltration of liquid such as water, alcohol, and LC to multiple air channels in the PCF structure is not of the same infiltration speed and, thus, of different infiltration length among the filled channels. Moreover, the infiltration in the channels is not continuous, i.e., there are intervals of unfilled regions or bubbles in the LC-filled channel that can be observed transversely under the microscope. In other words, it is difficult to ensure uniform infiltration among multiple air channels and to obtain a continuous infiltration in the channel without air gaps. Comparatively, selective infiltration of LC can provide better control in developing tunable devices for sensing applications. First, with selective infiltration to desirable air holes in the PCF structure, the number of filled air channels is controlled and reduced to single void in this work, which significantly circumvents the problem of nonuniform LC infiltration in multiple air holes. Second, the fabricated device is compact, i.e., around 9 mm; the presence of the bubbles in the filled channel is also greatly reduced due to shorter infiltration length. In this paper, we construct a compact directional PCF coupler by selectively filling nematic LC (NLC) 6CHBT (Military University of Technology, Warsaw, Poland) in a single void next to the silica core in the PCF. The device relies on mode couplings between the NLC channel guided modes and silica core modes, as reported in the directional coupler structures [20], [21]. A finite-difference method is employed to model the directional coupler structure and investigate the modal properties as well as coupling characteristics. The coupling characteristics and temperature response of the device are experimentally studied.

2. Operating Principle and Simulation Results

The operating principle of the LCPCF directional coupler is based on the mode couplings between the NLC-filled-channel guided modes and the silica core guided modes, which lead to transmission notches in the measured spectrum. The transmission notches occur at phase matching wavelengths where the effective mode indices of the NLC channel guided modes are equal to the silica core guided modes. The silica core guided modes are insensitive to varying temperature; on the other hand, due to the temperature dependence of the optical properties of the NLC, the effective mode indices of the NLC channel guided modes change significantly as a function of temperature. As a result, the phase matching wavelength corresponding to the transmission notch is a function of temperature, and the spectral shift of the transmission notch can be measured by an optical spectrum analyzer (OSA) to investigate the temperature response of the device.

The schematic diagram of the single-void-filled LCPCF directional coupler device is shown in Fig. 1. The LCPCF device is spliced to single-mode fiber (SMF) at both sides, which are connected to an amplified spontaneous emission broadband light source (1530–1600 nm) and OSA. The upper inset figure is the microscopic image of the cross section of the single-void-filled LCPCF. The NLC-filled void next to the silica core shows a white color that is different from the rest of the unfilled voids. The lower inset figure shows the splicing between SMF and LCPCF. The LCPCF device is placed in an oven with temperature control accuracy of 0.1 °C ranging from room temperature to 53 °C since the measurement of the refractive index (RI) of 6CHBT as a function of varying temperature is available in this range. The RI profile of 6CHBT as a function of temperature is plotted in Fig. 2. The transition from nematic phase to isotropic phase occurs at clearing temperature, i.e., 43 °C. The RI in nematic phase and isotropic phase are denoted by n_e, n_o, and n_{iso}, respectively. Because of the

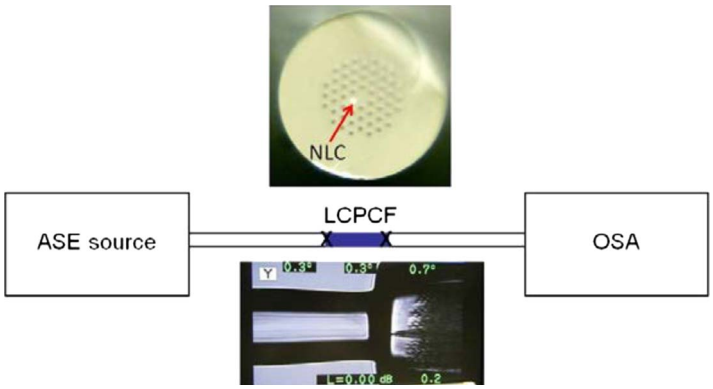

Fig. 1. Schematic diagram of the LCPCF-based directional coupler device. Inset: upper, the microscopic image of the single-void-filled LCPCF; lower, the splicing between the SMF and LCPCF.

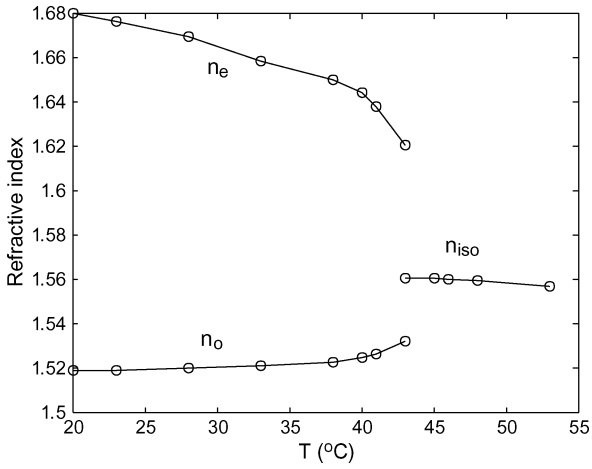

Fig. 2. Temperature dependence of the RI of the NLC used in the experiment.

predominated axial alignment of NLC molecule in the LCPCF, the effect of the birefringence is neglected in the simulation, and n_o is used as the RI below the clearing temperature.

The LCPCF directional coupler is modeled by the finite-difference method (Mode Solutions, Lumerical) for analysis of mode properties as well as its coupling characteristics. The PCF used in this work is an LMA-25 fiber from NKT Photonics. The diameter of the voids is 8.4 μm, the pitch is 16.35 μm, and the outer diameter is 268 μm. The RI of silica is assumed to be 1.448 and remains constant for different temperatures. The RI of the NLC is based on measurements shown in Fig. 2. It should be noted that the material dispersion of silica can be modeled by Sellmeier's equation, and that of NLC can be modeled by the equation with Cauchy coefficients [27]. However, as shown in [19], any slight deviation of the fabricated device from the simulated structure can lead to significant difference in phase matching wavelength of experiments from simulation results. On the other hand, the spectral shifts with varying temperature can be accurately modeled by the simulation. Therefore, it is useful to use simulation results qualitatively to investigate the mode properties of the directional coupler structure. Nevertheless, the coupling mechanism can be elucidated by the simulated effective mode index profiles, and the device sensitivity can be calculated by the simulations accurately. Therefore, the material dispersion for both silica and NLC is neglected in the simulations for simplicity without losing clarity on the analysis.

Because the RI of the NLC is much higher than that of silica, only NLC channel guided higher order modes can couple to silica core guided modes when their effective mode indices are equal.

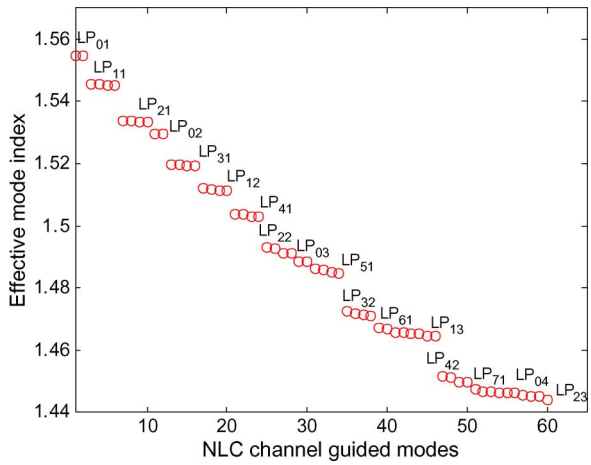

Fig. 3. Mode table of the NLC channel guided modes at temperature of 46 °C and wavelength of 1600 nm.

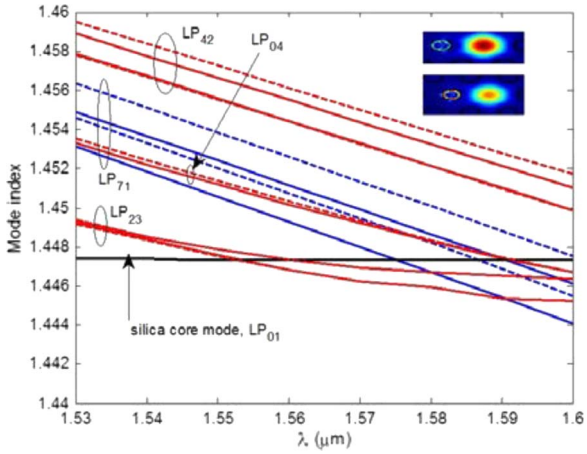

Fig. 4. Calculated effective mode indices of NLC channel guided modes LP_{42}, LP_{04}, LP_{71}, and LP_{23} and silica core guided mode LP_{01}.

The NLC channel guided modes up to the 60th mode at a wavelength of 1600 nm are calculated and plotted in Fig. 3 using the RI value at 46 °C for illustration. LP refers to linear polarized mode with degeneracy. The modes LP_{42}, LP_{04}, LP_{71}, and LP_{23} are likely to intersect with the silica core guided modes, i.e., the LP_{01} mode of the silica core modes is considered. The effective mode indices of the aforementioned NLC channel guided modes and silica core guided mode LP_{01} are calculated as a function of wavelength and shown in Fig. 4. Apparently, there are intersections between the NLC guided mode index curves and silica core mode curve, indicating the likely occurrence of mode couplings between both waveguides. The mode couplings are very wavelength dependent because the curves do not overlap across a broad wavelength window, which leads to narrow full-width half-maximum of the transmission notch and will be verified by experimental measurements. Furthermore, there are multiple NLC channel guided modes intersecting the silica core guided mode. Each coupling takes place at different phase matching wavelengths, and the mode profiles as well as the coupling length are thus different. For instance, the odd and even modes representing the likely mode coupling between the LP_{71} mode and the LP_{01} mode are shown in the inset figure. The phase matching wavelength is at 1575 nm, and the coupling length is 5.2 cm. Although the phase match wavelength determined by positioning the intersection wavelength

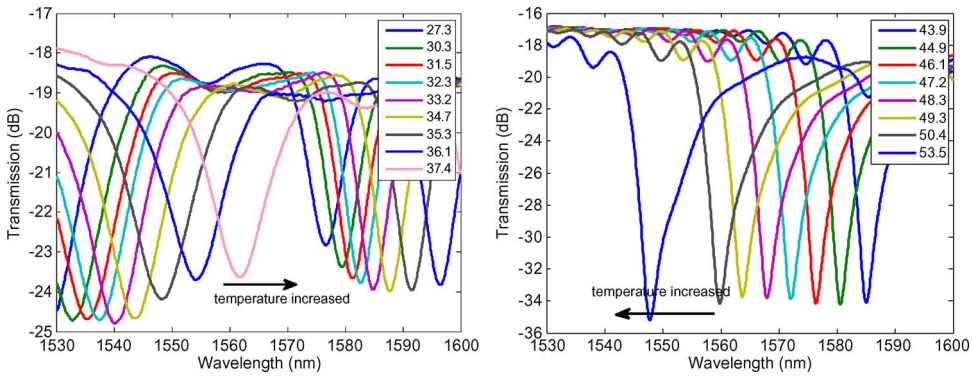

Fig. 5. Measured transmission spectra at temperature range (a) from 27.3 °C to 37.4 °C in nematic phase of NLC and (b) from 43.9 °C to 53.5 °C in isotropic phase of NLC.

on the mode index curves can be significantly different from the actual experiment [19], the spectral shift of the phase matching wavelength can be calculated by the simulation accurately. Next, the lowest order mode of the degenerate LP_{71} mode is simulated at temperature values of 48 °C and 53 °C, where the RI of NLC is available, showing spectral shifts of 7 and 23 nm, respectively [24]. The spectral shift can be a linear fit with sensitivity of -3.30 nm/°C.

3. Fabrication and Measurements

The PCF is blocked by liquid glue, leaving only one void open for NLC infiltration. After the glue dries, the blocked side of the PCF is placed into the 6CHBT solution, allowing the LC to infiltrate the unblocked void *via* capillary effect. The infiltration pattern is verified by observing the other side of the PCF under microscope, as shown in Fig. 1. This confirms that the NLC is filled only in one void shown in white color, and the infiltration is up to the entire length of the PCF. Both sides of the PCF are cleaved and spliced to SMF using a fusion arc splicer. The fabricated LCPCF device length is about 0.9 cm. The PCF device is placed in an oven, and the temperature is varied while the device spectrum is monitored.

The measured spectra are plotted in Fig. 5, which shows the transmission profile from 27.3 °C to 37.4 °C in nematic phase of NLC and from 43.9 °C to 53.5 °C in isotropic phase of NLC. First, there are two obvious notches in the transmission spectrum in nematic phase, and they show steady red shifts to longer wavelengths as temperature increases. Second, the transmission spectrum in isotropic phase only exhibits one deep notch that moves to shorter wavelengths as temperature rises. The extinction ratio is about 17 dB, and the full-width half-maximum of the transmission dips is narrow, i.e., approximately 2 nm, which is highly desirable for sensing purposes. This is in line with the temperature dependence of the NLC RI shown in Fig. 2. Therefore, by measuring the spectral positions of the notches, i.e., the resonance wavelengths, we can characterize the temperature sensitivity of the LCPCF-based directional coupler device, as shown in Fig. 6. The temperature response curves of the two notches of the spectra in nematic phase can be well fitted by second-order polynomial curves. On the other hand, the linear line fits well to the measured resonance wavelength in isotropic phase of NLC associated with temperature sensitivity of -3.86 nm/°C. Compared with earlier demonstrated fluid-filled PCF directional coupler with temperature sensitivities of 11.61 nm/°C and 54.3 nm/°C and temperature measurement windows of 1 °C and 1.5 °C [20], [21], the achieved sensitivity is lower, but the temperature measurement window of the demonstrated device in this work extends from the nematic phase to the isotropic phase of the NLC, i.e., we demonstrated temperature sensing from 27 °C to 54 °C with a distinctively different spectrum for detection. In addition, the achieved sensitivity is much higher than grating-based temperature sensors ($\sim$0.01 nm/°C) [9]. The demonstrated device is desirable to be used as a point sensor. On the other hand, the temperature range that the NLC-filled PCF coupler device can be used depends on the properties of the NLC and may not be feasible for high-temperature

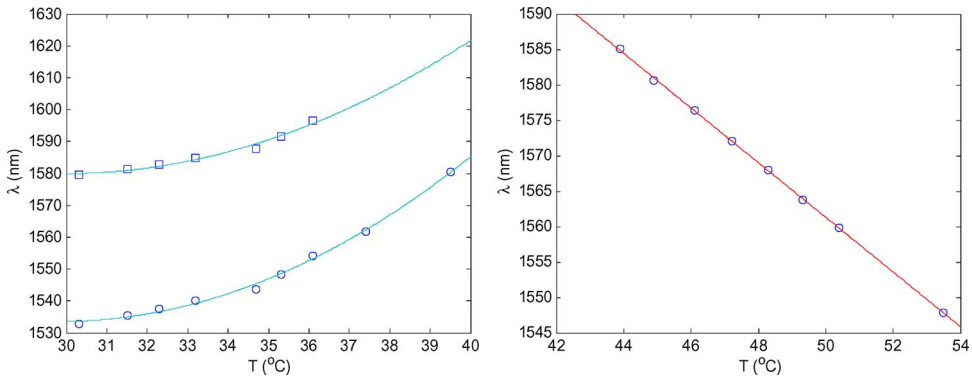

Fig. 6. Dip wavelength of the device shows linear blue-shifts with varying temperature from 43.9 °C to 53.5 °C.

sensing. In this paper, we only tested temperature up to 54 °C up to which the RI profile of the NLC is available.

4. Conclusion

In conclusion, the compact directional coupler structure based on PCF filled with NLC is investigated both theoretically and experimentally. The guided modes of the NLC waveguide are examined for coupling with silica core waveguide. The coupling characteristics are demonstrated experimentally, and the transmission spectra exhibit detectable notches for temperature sensing applications.

Acknowledgment

The authors would like to thank Prof. R. Dabrowski and Dr. E. Nowinowski-Kruszelnicki of Military University of Technology, Warsaw, Poland, for supplying the liquid crystal material.

References

[1] J. M. Dudley and J. R. Taylor, "Ten years of nonlinear optics in photonic crystal fibre," *Nat. Photon.*, vol. 3, no. 2, pp. 85–90, Feb. 2009.
[2] A. Urich, R. R. J. Maier, B. J. Mangan, S. Renshaw, J. C. Knight, D. P. Han, and J. D. Shephard, "Delivery of high energy Er:YAG pulsed laser light at 2.94 μm through a silica hollow core photonic crystal fibre," *Opt. Exp.*, vol. 20, no. 6, pp. 6677–6684, Mar. 2012.
[3] N. Anscombe, "Photonic crystal pioneer," *Nat. Photon.*, vol. 5, no. 8, pp. 464–465, Aug. 2011.
[4] D. J. J. Hu, P. Shum, C. Lu, X. Yu, G. Wang, and G. Ren, "A holey fiber design for single-polarization single-mode guidance," *Appl. Opt.*, vol. 48, no. 20, pp. 4038–4043, Jul. 2009.
[5] D. J. J. Hu, P. Shum, C. Lu, and G. Ren, "Dispersion-flattened polarization-maintaining photonic crystal fiber for nonlinear applications," *Opt. Commun.*, vol. 282, no. 20, pp. 4072–4076, Oct. 2009.
[6] D. J. J. Hu, G. Alagappan, Y. K. Yeo, P. P. Shum, and P. Wu, "Broadband transmission in hollow-core Bragg fibers with geometrically distributed multilayered cladding," *Opt. Exp.*, vol. 18, no. 18, pp. 18 671–18 684, Aug. 2010.
[7] A. M. R. Pinto and M. Lopez-Amo, "Photonic crystal fibers for sensing application," *J. Sensors*, vol. 2012, pp. 598178-1–598178-21, 2012.
[8] D. J. J. Hu, J. L. Lim, M. K. Park, L. T.-H. Kao, and Y. Wang, "Photonic crystal fiber based interferometric biosensor for streptavidin and biotin detection," *IEEE J. Sel. Topics Quantum Electron.*, vol. 18, no. 4, pp. 1293–1297, Jul./Aug. 2012.
[9] D. J. J. Hu, J. L. Lim, M. Jiang, Y. Wang, F. Luan, P. P. Shum, H. Wei, and W. Tong, "Long period grating cascaded to photonic crystal fiber modal interferometer for simultaneous measurement of temperature and refractive index," *Opt. Lett.*, vol. 37, no. 12, pp. 2283–2285, Jun. 2012.
[10] J. L. Lim, D. J. J. Hu, P. P. Shum, and Y. Wang, "Cascaded photonic crystal fiber interferometers for refractive index sensing," *IEEE Photon. J.*, vol. 4, no. 4, pp. 1163–1169, Aug. 2012.
[11] K. Nielsen, D. Noordegraaf, T. Srensen, A. Bjarklev, and T. P. Hansen, "Selective filling of photonic crystal fibres," *J. Opt. A, Pure Appl. Opt.*, vol. 7, no. 8, pp. L13–L20, Aug. 2005.
[12] A. M. Jones, A. V. V. Nampoothiri, A. Ratanavis, T. Fiedler, N. V. Wheeler, F. Couny, R. Kadel, F. Benabid, B. R. Washburn, K. L. Corwin, and W. Rudolph, "Mid-infrared gas filled photonic crystal fiber laser based on population inversion," *Opt. Exp.*, vol. 19, no. 3, pp. 2309–2316, Jan. 2011.

[13] Y. Cui, P. P. Shum, D. J. J. Hu, G. Wang, G. Humber, and Q. Dinh, "Temperature sensor by using selectively-filled photonic crystal fiber Sagnac interferometer," *IEEE Photon. J.*, vol. 4, no. 5, pp. 1801–1808, Oct. 2012.
[14] H. W. Lee, M. A. Schmidt, and P. St. J. Russell, "Excitation of a nanowire 'molecule' in gold-filled photonic crystal fiber," *Opt. Lett.*, vol. 37, no. 14, pp. 2946–2948, Jul. 2012.
[15] N. Healy, J. R. Sparks, R. R. He, P. J. A. Sazio, J. V. Badding, and A. C. Peacock, "High index contrast semiconductor ARROW and hybrid ARROW fibers," *Opt. Exp.*, vol. 19, no. 11, pp. 10 979–10 985, May 2011.
[16] B. T. Kuhlmey, B. J. Eggleton, and D. K. C. Wu, "Fluid-filled solid-core photonic bandgap fibers," *J. Lightw. Technol.*, vol. 27, no. 11, pp. 1617–1630, Jun. 1, 2009.
[17] C. Kerbage, P. Steinvurzel, P. Reyes, P. S. Westbrook, R. S. Windeler, A. Hale, and B. J. Eggleton, "Highly tunable birefringent microstructured optical fiber," *Opt. Lett.*, vol. 27, no. 10, pp. 842–844, May 2002.
[18] C. Kerbage and B. Eggleton, "Numerical analysis and experimental design of tunable birefringence in microstructured optical fiber," *Opt. Exp.*, vol. 10, no. 5, pp. 246–255, Mar. 2002.
[19] M. Vieweg, T. Gissibl, S. Pricking, B. T. Kuhlmey, D. C. Wu, B. J. Eggleton, and H. Giessen, "Ultrafast nonlinear optofluidics in selectively liquid-filled photonic crystal fibers," *Opt. Exp.*, vol. 18, no. 24, pp. 25 232–25 240, Nov. 2010.
[20] D. K. C. Wu, B. T. Kuhlmey, and B. J. Eggleton, "Ultrasensitive photonic crystal fiber refractive index sensor," *Opt. Lett.*, vol. 34, no. 3, pp. 322–324, Feb. 2009.
[21] Y. Wang, M. Yang, D. N. Wang, and C. R. Liao, "Selectively infiltrated photonic crystal fiber with ultrahigh temperature sensitivity," *IEEE Photon. Technol. Lett.*, vol. 23, no. 20, pp. 1520–1522, Oct. 2011.
[22] F. Du, Y. Lu, and S.-T. Wu, "Electrically tunable liquid-crystal photonic crystal fiber," *Appl. Phys. Lett.*, vol. 85, no. 12, pp. 2181–2183, Sep. 2004.
[23] T. R. Wolinski, A. Czapla, S. Ertman, M. Tefelska, A. W. Domanski, J. Wojcik, E. Nowinowski-Kruszelnicki, and R. Dabrowski, "Photonic liquid crystal fibers for sensing applications," *IEEE Trans. Instrum. Meas.*, vol. 57, no. 8, pp. 1796–1802, Aug. 2008.
[24] D. J. J. Hu, J. L. Lim, Y. Cui, K. Milenko, Y. Wang, P. Shum, and T. Wolinski, "Fabrication and characterization of a highly temperature sensitive device based on nematic liquid crystal-filled photonic crystal fiber," *IEEE Photon. J.*, vol. 4, no. 5, pp. 1248–1255, Oct. 2012.
[25] J. J. Hu, G. Ren, P. Shum, X. Yu, G. Wang, and C. Lu, "Analytical method for band structure calculation of photonic crystal fibers filled with liquid crystal," *Opt. Exp.*, vol. 16, no. 9, pp. 6668–6674, Apr. 2008.
[26] G. Ren, P. Shum, J. Hu, X. Yu, and Y. Gong, "Study of polarization-dependent bandgap formation in liquid crystal filled photonic crystal fibers," *IEEE Photon. Technol. Lett.*, vol. 20, no. 8, pp. 602–604, Apr. 2008.
[27] J. Li, S. Wu, S. Brugioni, R. Meucci, and S. Faetti, "Infrared refractive indices of liquid crystals," *J. Appl. Phys.*, vol. 97, no. 7, pp. 073501-1–073501-5, Apr. 2005.